Journal of Radiation Research, Vol. 61, No. 1, 2020, pp. 58–67
doi: 10.1093/jrr/rrz076
Advance Access Publication: 17 December 2019

The influence of Geant4-DNA toolkit parameters on electron microdosimetric track structure

Yidi Wang[1,2,3], Zhanpeng Li[1,2,3], Shuyuan Zhang[1,2,3], Wei Tang[1,2,3], Xiang Li[1,2,3], Dandan Chen[1,2,3] and Liang Sun[1,2,3,*]

[1]School of Radiation Medicine and Protection, Medical College of Soochow University, Suzhou 215123, China
[2]State Key Laboratory of Radiation Medicine and Protection, Suzhou 215123, China
[3]Collaborative Innovation Centre of Radiation Medicine of Jiangsu Higher Education Institutions, Suzhou 215123, China
*Corresponding author. Dushuhu Campus, Soochow University, No. 199, Ren'ai Road, Suzhou Industrial Park(SIP), Suzhou City, Jiangsu Province, PRC. Email: slhmz666@suda.edu.cn
(Received 26 July 2019; revised 19 September 2019; editorial decision 3 October 2019)

ABSTRACT

The influence of different physical process factors on tracks of low-energy electrons in liquid water was analyzed and evaluated based on the Geant4-DNA toolkit of Geant4 version 10.4, and it provides theoretical support for obtaining the basic parameters of microdosimetry concerned with radiotherapy and radiation protection. According to the characteristics of different models, five physics constructors of Geant4-DNA toolkit were selected to simulate monoenergetic electrons in microscopic scale. Details of track structure of different Geant4-DNA physics constructors were compared, including total number of interaction processes, number and energy percentage of excitation and ionization; analyzing the impacts of mean lineal energy of several factors, including Geant4-DNA physics constructors, initial energy, radius of scoring spheres, interaction processes and cut-off energy. Firstly, 'G4EmDNAPhysics' (hereinafter referred to as 'dna') is well consistent with 'G4EmDNAPhysics_option 2' (hereinafter referred to as 'option 2'), and 'G4EmDNAPhysics_option 4' (hereinafter referred to as 'option 4') is well consistent with 'G4EmDNAPhysics_option 5' (hereinafter referred to as 'option 5'); secondly, there are differences for the information of track structure and mean lineal energy between 'option 2' 'option 4' and 'G4EmDNAPhysics_option 6' (hereinafter referred to as 'option 6'); thirdly, the influence of the model on the mean lineal energy decreases with the increase of the radius of the scoring spheres, whereas mean lineal energy increases as the tracking cut increases. Several alternative discrete physics constructors of Geant4-DNA are comprehensively discussed overlaying multiple perspectives under different conditions in this work.

Keywords: Monte Carlo; Geant4-DNA; microdosimetry; track structure

INTRODUCTION

Low-energy electrons are ubiquitous in the medium or environment under all kinds of irradiation conditions of radiotherapy and radiation protection [1]. The fraction of biological effects depends on particle and that of energy, and the vast majority (over 90%) of biological effects, such as DNA molecular strand breaks, are caused by secondary electrons generated by high-energy primary ionizing radiation [2, 3]. The cellular and subcellular levels of low-energy electrons at the biological tissues are also likely to produce highly localized energy deposition and ionization groups [4]. Since DNA is the most radiosensitive target in cells, the track structure of low-energy electrons and DNA damage have a close relationship when studying the relationship between radiation quality and biological effects [4–8]. Nikjoo et al. had a review of the recent development in the physics of radiation track structure, and hypothesized that radiation physics, with mathematical modeling, can help elucidate biological mechanisms and cancer therapies [9].

Indicators of macroscopic dosimetry like linear energy transfer (LET) and absorbed dose can reflect the mean level, yet they are limited when reflecting the randomness of interaction between radiation and matter in the target region [10]. In the practical work scenarios of radiotherapy and radiation protection, the energy

deposition distribution generated by particle tracks in the micro volume is described by two random physical quantities in microdosimetry, i.e. line energy y and specific energy z, instead of linear energy transfer and absorbed dose when the target size is small enough, and dose mean lineal energy $\bar{y}_D$ is considered to be an effective physical quantity for evaluating biological effects [11]. On the other hand, tissue equivalent proportional counter (TEPC) is the main detector in the microdosimetry research [12], Borak et al. [13] have performed some experiments to measure the response of TEPC and a silicon-based LET spectrometer (RRMD-III) to protons with energies ranging from 50–200 MeV. Rollet et al. [14] have shown comparisons for photons between simulations using the Monte Carlo FLUKA and experimental data in a mini TEPC (with sizes equivalent to 1 and 2 um). A silicon-on-insulator (SOI) process for pixelated radiation detectors has been developed and its good sensitivity has been confirmed [15], the target size was at the micron scales and the energy of X-ray was 8 keV. Because the penetration ability of low-energy electrons is poor, and the sensitive volume of TEPC is at the micron scale, it is difficult to measure the microdosimetric parameters of low-energy electrons directly with current technology, and at the nanometer scale it can only be obtained by means of Monte Carlo simulation. Geant4 [16–18] is a Monte Carlo application toolkit based on C++ object-oriented technology. Geant4-DNA toolkit allows an event-by-event description of physical electromagnetic interactions of particles down to eV scale and track structure simulation of spaces similar in size to biological targets [19].

There are lots of researches on energy deposition in microscopic volumes [7, 10, 20–27]: Emfietzoglou et al. [28] discussed the impacts of physics on inelastic scattering and electron track structure, and stressed the importance of physics models in microdosimetry. Kyriakou et al. [29] found that the development of physics models in the Geant4-DNA extension would affect those applications where the spatial pattern of interactions and energy deposition of very-low energy electrons play an important role. Kyriakou et al. [30] pointed out the applicability of the Geant4-DNA toolkit to microdosimetric simulations by calculating the microdosimetric energy spectrum of electrons in liquid water, whereas condensed-history codes may yield reasonable results for sites as small as a few tens of a nanometer with appropriate simulation parameters. Microdosimetric quantities are very sensitive to the choice of physics model, target size and user-defined simulation parameters. There has been systematic comparison between condensed history and track structure models for users choosing suitable physics model in the simulations [31, 32]. Most of the other papers are concerned with the value and distribution of the lineal energy and the specific energy of the microscopic volume, lacking a complete analysis of the track, especially the horizontal comparison of models under different physical process settings.

Radiation track is composed of energy transfer points in the process of interaction between particle and material. The key information required for tracking particle transport records, including the location of the transfer point (three-dimensional coordinates), the energy of local deposition, and their type of interaction process. At present, Geant4-DNA is an important tool for studying microdosimetry, because all the processes in Geant4-DNA are discrete, which can simulate the physical process of each step in the track using condensed-history techniques. We analyzed the impacts of physical constructors, radius of scoring spheres, interaction processes and cut-off energy on frequency mean lineal energy $\bar{y}_F$ and dose mean lineal energy $\bar{y}_D$ of electrons in liquid water; the track structure information is calculated by self-programmed MATLAB code, which includes the total number of interaction processes, number and energy percentage of excitation and ionization.

METHODS

Geant4-DNA toolkit and physical constructors

Table 1 lists the seven alternative models included in the Geant4-DNA toolkit and their shortened form in this paper, including three recommended models and the other four models.

Table 2 summarizes the cross-section models of electron interactions and other information of the three reference Geant4-DNA physics constructors. It mainly includes elastic scattering and inelastic interactions, namely electronic excitation and ionization. In addition, 'option 2' considers vibrational excitation and attachment as well, which are suitable for electrons that do not have enough kinetic energy to withstand electron excitation and ionization [33, 34]. Furthermore, there is a Geant4-DNA process for the cut-off energy of the track called 'G4DNAElectronSolvation', it does not apply when chemistry simulation is activated because electrons are tracked till thermalization and are considered as solvated [19], it will not be discussed in this paper.

Other physics constructors have been provided historically with Geant4-DNA: 'dna' is the default model for the initial Geant4-DNA toolkit, its elastic scattering and ionization process are slower than 'option 2'; the electron elastic scattering cross section model of 'option 1' is a low-energy extension of the original 'WentzelVI' [35], this model has not been validated and is currently provided as a beta development only [36]; 'option 3' is obsolete. Geant4 10.5, updated in December 2018, did not significantly modify the Geant4-DNA toolkit for electron transport in liquid water.

According to the characteristic of different Geant4-DN physics constructors, 'dna', 'option 2', 'option 4', 'option 5' and 'option 6' were selected in this work.

Geometric environment and operating conditions

Electrons with designated incident energy are placed in a box filled with liquid water, electrons are emitted in the same direction. Fig. 1 shows a single track structure image of 1 keV monoenergetic electron in liquid water. Red represents negative charged.

Lineal energy y is defined as the ratio $\varepsilon/\bar{l}$ where ε is the deposited energy by a single particle track in the site and $\bar{l}$ is the mean chord length of the volume. Specific energy z is defined as the ratio ε/m where m is the mass of the site. For a single event, specific energy and lineal energy can be converted mutually by coefficients. Therefore, when comparing the track structure differences simulated by different physical models for a single event, we only need to compare one of them. Frequency mean lineal energy $\bar{y}_F = \int_0^\infty \mathrm{yf}(\mathrm{y})\,\mathrm{dy}$, where $\mathrm{f}(\mathrm{y})$ is the probability density function of lineal energy y. Dose mean lineal energy $\bar{y}_D = \int_0^\infty y\mathrm{d}(y)\,\mathrm{d}y = \frac{1}{\bar{y}_F}\int_0^\infty y^2 f(y)\,\mathrm{d}y$, where $\mathrm{d}(\mathrm{y}) = \mathrm{yf}(\mathrm{y})/\bar{y}_F$ is introduced as the dose probability density function of lineal energy.

It is necessary to set a threshold, so-called 'the cut-off energy', for the particle simulation in view of the time and calculation accuracy.

Table 1. The collection of Geant4-DNA toolkit in Geant4 10.4

	Geant4-DNA alternative models	Shortened form
Recommended models	'G4EmDNAPhysics_option 2'	'option 2'
	'G4EmDNAPhysics_option 4'	'option 4'
	'G4EmDNAPhysics_option 6'	'option 6'
Other models	'G4EmDNAPhysics'	'dna'
	'G4EmDNAPhysics_option 1'	'option 1'
	'G4EmDNAPhysics_option 3'	'option 3'
	'G4EmDNAPhysics_option 5'	'option 5'

Table 2. The information on the three reference Geant4-DNA physics constructors for TS (track structure) simulations of electrons in liquid water available in the Geant4 10.4 release [19]

	'option 2' (Default)	'option 4' (Ioannina)	'option 6' (CPA100)
Elastic scattering	Partial wave model[36]	Uehara screened Rutherford model[37]	Independent Atom Method model from CPA100 code[33]
Electronic excitation	Emfietzoglou dielectric model[38, 39]	Emfietzoglou–Kyriakou dielectric model[29, 37, 38]	Dielectric model from CPA100 code[33, 34]
Ionization	Emfietzoglou dielectric model[38, 39]	Emfietzoglou–Kyriakou dielectric model[29, 37, 38]	Relativistic binary encounter Bethe model from CPA100 code[33, 34]
Default cut-off energy	7.4 eV	10 eV	11 eV
Maximum energy	1 MeV	10 keV	256 keV
Year of the release and Geant4 version	2007 Geant4 9.1	2016 Geant4 10.2	2017 Geant4 10.4

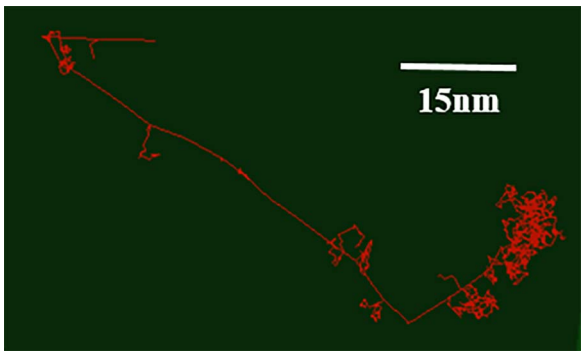

Fig. 1. A single track structure image of 1 keV monoenergetic electron in liquid water.

There are two types of cut-off energy that are commonly used, namely, tracking cut and production cut. Tracking cut is an absolute cut-off of the track. When the energy down to this value, the particles stop transporting and the remaining energy is released locally. Production cut means that when the energy is less than this value, secondary particles are no longer produced. Geant4-DNA toolkit sets the default tracking cut for each model.

A single particle track is a collection of energy deposition locations of individual ionized particles and their secondary particles in the material. Kellerer proposed a weighted sampling to obtain a microdosimetric spectra [40]. This method can obtain an accurate inefficient dose distribution. Kyriakou et al. [30] sampled sites by the number of interaction and weighting factor of electron energy. We used the same sampling method as Kyriakou et al., scoring spheres of diameters relevant to sub-cellular biological targets were chosen: DNA base pair (2 nm), nucleosome (10 nm), chromatin fiber (30 nm), and chromosome (300 nm).

RESULTS AND DISCUSSION

17 incident electron energies were examined for 'dna', 'option 2' and 'option 6': 0.1, 0.2, 0.3, 0.4, 0.5, 0.7, 1, 2, 3, 5, 7, 10, 20, 50, 100, 150, 200 keV. Due to the limit of maximum energy, the energies below 10 keV are selected for 'option 4' and 'option 5', that is to say, 10 energies for both constructors. All simulations in the present work were performed by Geant4 10.4. The tracking cut was set to 11 eV unless otherwise specified. Considering the difference of the interaction process of different models, for the sake of comparison completeness, we discussed the influence of the elastic scattering, vibrational excitation and attachment in the physics constructors respectively. In the following illustration, if there is a certain operating condition 'inelastic scattering', it means that elastic scattering in the process is not considered; if 'no attachment and vibexcitation' occurs, it means that elastic scattering, vibrational excitation and attachment are not considered.

Table 3. Mean energy of single energy deposition of excitation and ionization (IU: eV)

	Excitation	Ionization
'dna'	10.35±0.29	12.89±0.42
'option 2'	10.37±0.31	12.88±0.46
'option 4'	9.76±0.08	12.78±0.49
'option 5'	9.72±0.12	12.71±0.55
'option 6'	10.72±0.29	13.94±0.42

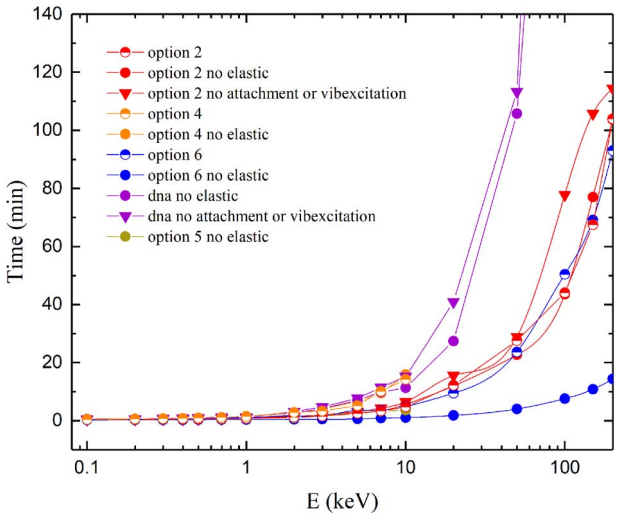

Fig. 2. The computing time for 10^6 monoenergetic electrons in liquid water using different Geant4-DNA physics constructors.

Computing time

In order to compare the computational efficiency of different models, an incident statistic of 10^6 electrons in liquid water was selected for incident energies using the same device, and the computation time was recorded. Simulations were performed by a high performing computer with an Intel(R) Xeon(R) E5–2696 2.2 GHz CPU, 256 GB RAMs and the CentOS7 LTS 64 bits operational system, using 16 threads for parallel computing. As shown in Fig. 2, the computing time for all the 10^6 electrons of 'dna' is the longest, while the computing time of 'option 4' is longer than 'option 5'. If vibrational excitation and attachment of 'dna' and 'option 2' are not considered, the computing time will increase; elastic scattering has little effect on the operation time of 'dna', 'option 2' and 'option 4', this may be related to the absence of energy loss of elastic scattering in the three models, whereas the total computing time of 'option 6' is greatly reduced, indicating that the simulation of elastic scattering accounts for the most of 'option 6' electron simulations.

Number and energy of interaction

In order to avoid the error caused by the randomness of interaction, the track of 10 monoenergetic electrons in liquid water was recorded by a single-threaded simulation, the corresponding information of the single track was obtained after averaging the statistics of the track structure files.

The total number of interaction processes of different models is basically the same, the number of 'dna' and 'option 2' is consistent, slightly smaller than 'option 6'; The number of energy depositions for the excitation and ionization of each model (regardless of elastic scattering, vibrational excitation, and attachment) is consistent. Fig. 3 shows number and energy percentage of excitation and ionization for monoenergetic electrons in liquid water of different physics constructors. Fig. 3(a) summarizes proportion of number of excitations and ionizations, and Fig. 3(b) summarizes proportion of energy deposited in the interaction process by monoenergetic electrons. As shown, the number and energy percentage of excitation of each model are lower than ionization. 'option 4' and 'option 5' have lower ionization number and deposited energy percentage than other models, whereas their excitation number and deposited energy percentage are higher than other models, and the average deposited energy of 'option 4' and 'option 5' excitation is the smallest compared to other physical processes, which have been confirmed by Kyriakou I et al. [37]. This is because 'option 4' and 'option 5' change the dielectric function for calculating the inelastic scattering interaction cross section compared to other models, so that the ionization cross section is moderately reduced and the excitation cross section is enhanced significantly. The number and energy percentage of 'option 6' excitation is slightly larger than 'dna' and 'option 2'. The proportion of ionization number is slightly smaller than 'dna' and 'option 2', but the ratio of ionization energy is larger than 'dna' and 'option 2'. One reason is that the average deposited energy of the 'option 6' ionization is the highest of all models, which is 13.94 eV. The ionization and excitation average deposited energy of other models are shown in Table 3.

It is found that there are two energy transfer points with different interaction processes, different deposited energy but with identical coordinates. The number of transfer points with overlapping coordinate accounts for about 5% of the total interaction process, and the high energy portion of 'option 2' and 'option 6' is larger than other cases. The main reason is that the kinetic energy falls to below tracking cut after the ionization and excitation process, leading to locally deposited electrons, and the elastic scattering transfer point is large in quantity.

Frequency mean lineal energy and dose mean lineal energy

Fig. 4 summarizes frequency mean lineal energy of monoenergetic electrons in different radius point of each model. Fig. 4(a) (c) (d) only

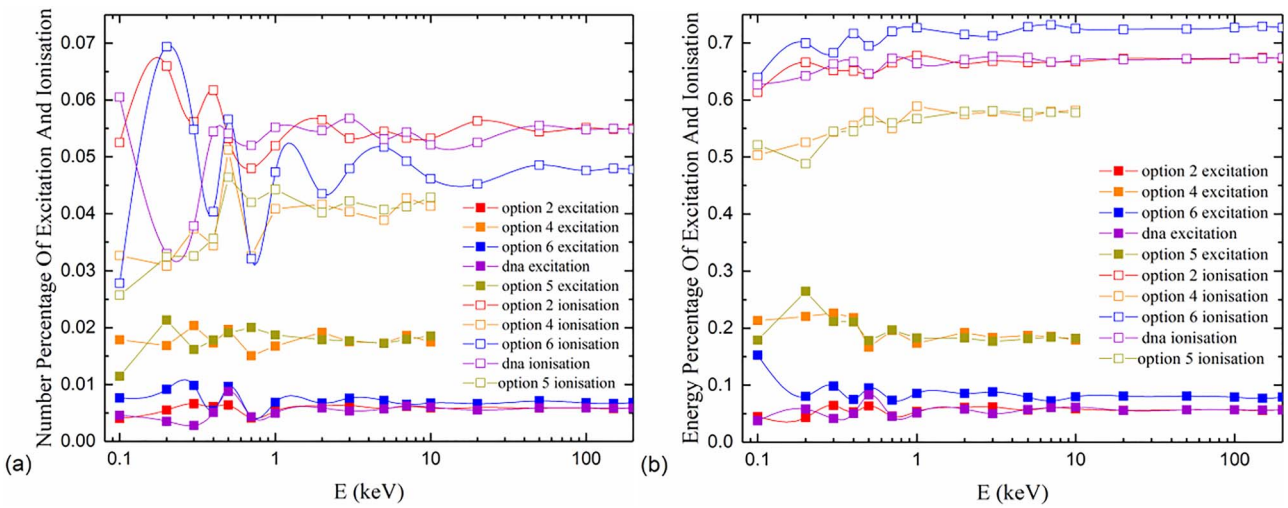

Fig. 3. Proportion of number (a) and energy (b) of excitation and ionization by monoenergetic electrons in liquid water using different Geant4-DNA physics constructors, and 'option 2 excitation' and 'option 2 ionisation' are the results without attachment or vibexcitation.

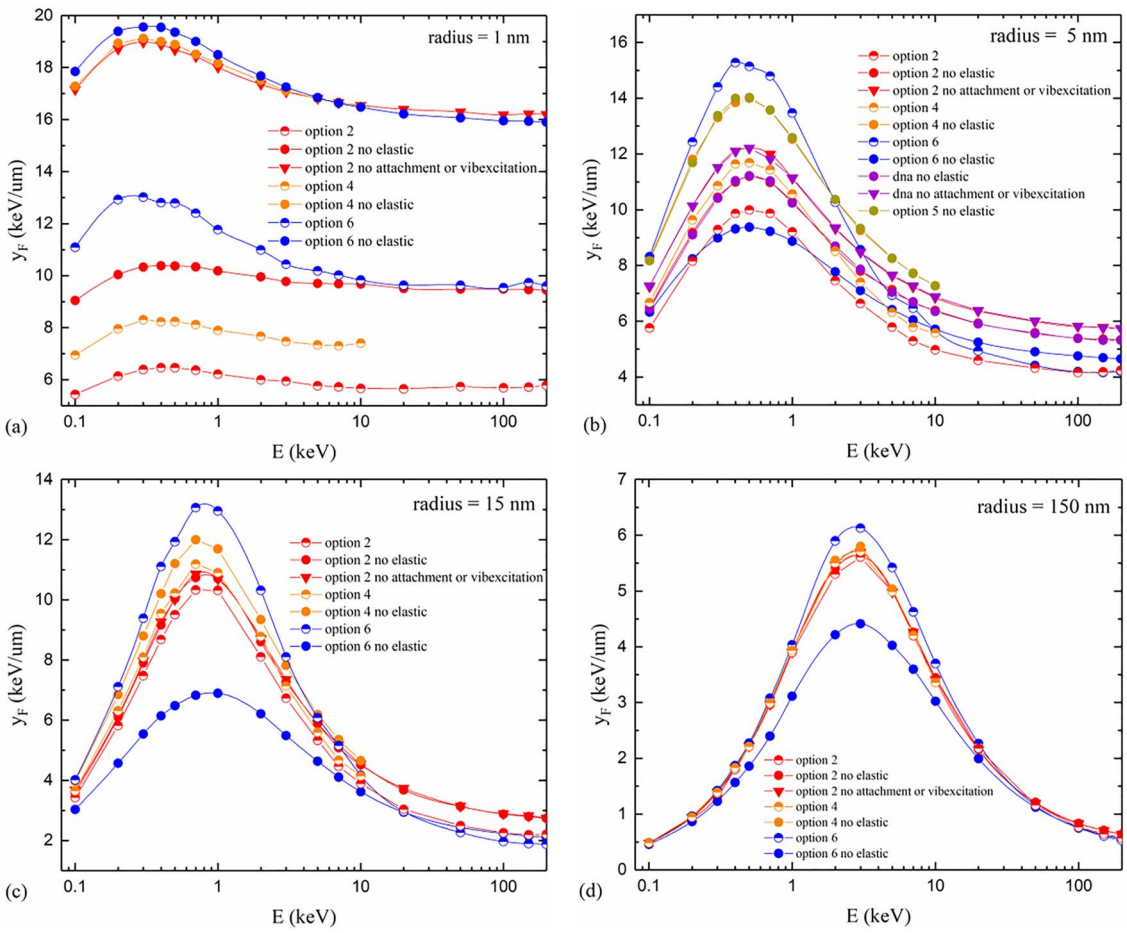

Fig. 4. Frequency mean lineal energy $\bar{y}_F$ as a function of monoenergetic electrons using different Geant4-DNA physics constructors,in scoring spheres with radius: 1 nm (a), 5 nm (b), 15 nm (c) and 150 nm (d).

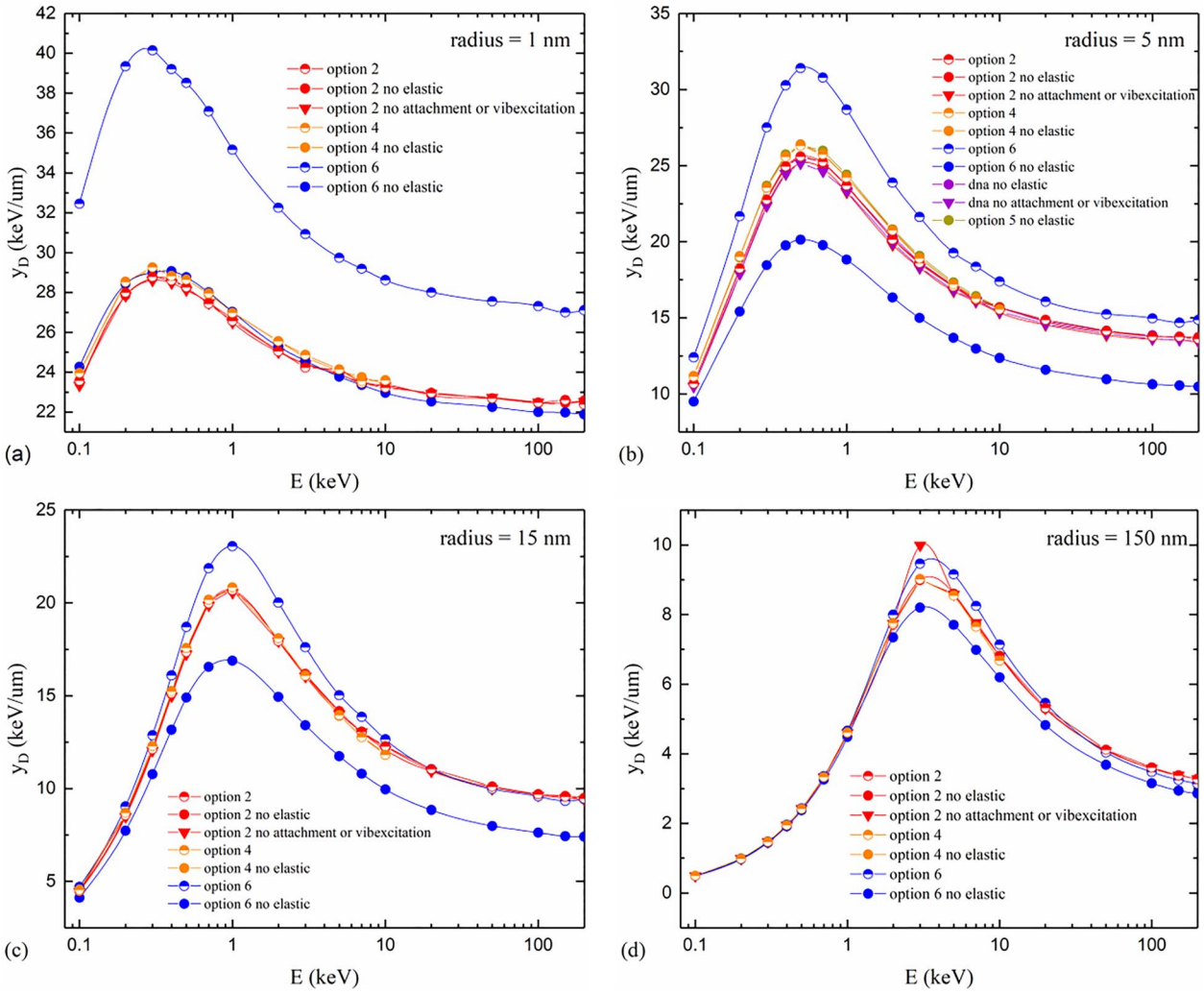

Fig. 5. Dose mean lineal energy $\bar{y}_D$ as a function of monoenergetic electrons using different Geant4-DNA physics constructors,in scoring spheres with radius: 1 nm (a), 5 nm (b), 15 nm (c) and 150 nm (d).

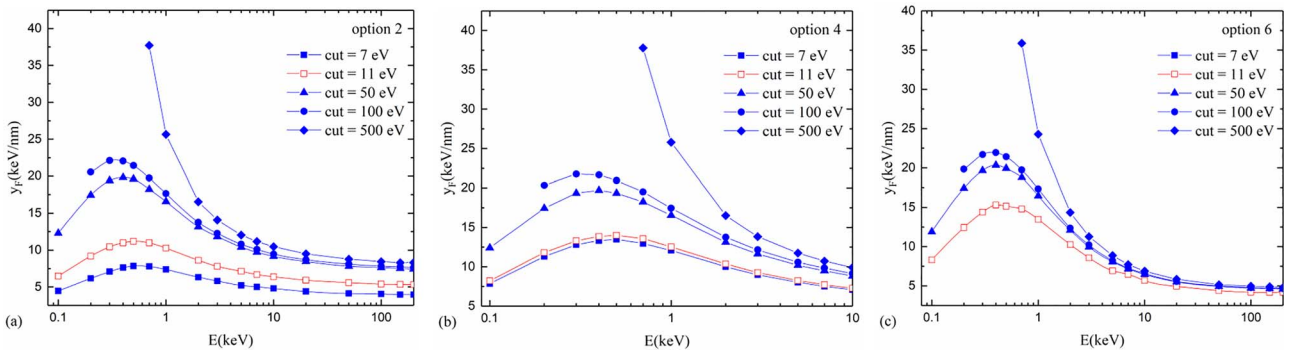

Fig. 6. Dose mean lineal energy $\bar{y}_D$ as a function of monoenergetic electrons in scoring spheres of 5 nm for different tracking cuts, using different Geant4-DNA physics constructors 'option 2' (a), 'option 4' (b), 'option 6' (c).

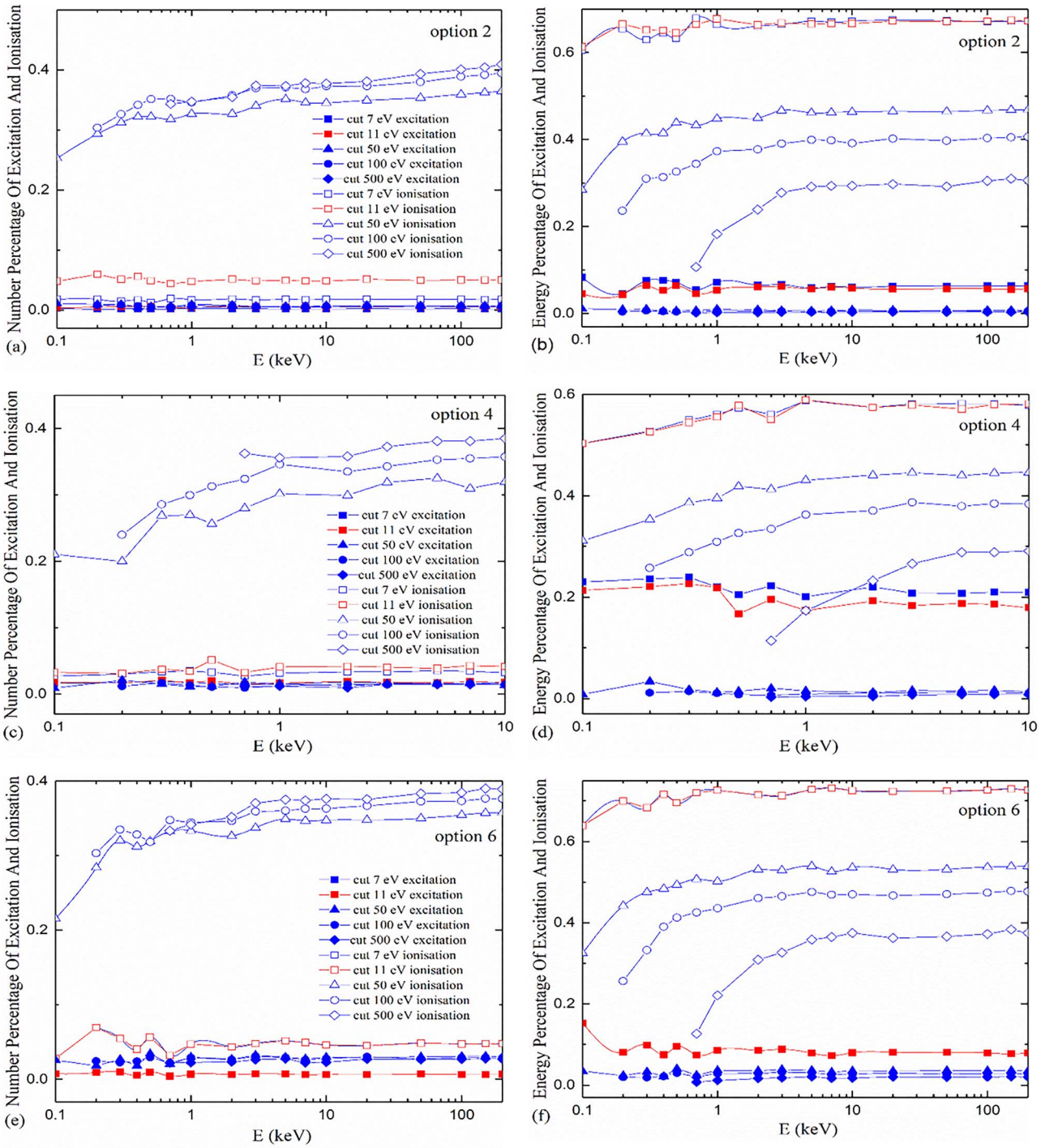

Fig. 7. Proportion of number (a) (c) (e) and energy (b) (d) (f) of excitation and ionization for monoenergetic electrons in liquid water for different tracking cuts, and (a) (b) corresponds to 'option 2', (c) (d) corresponds to 'option 4', (e) (f) corresponds to 'option 6'.

summarizes the mean values of 'option 2', 'option 4' and 'option 6', the frequency mean lineal energy of 'dna' and 'option 5' are also calculated in fig. 4 (b). If the conditions are the same, the calculation results in this work are virtually equal to [30], with a relative error of lower than 3%. The mean distribution trends of different models are basically the same. The larger radius, the smaller difference in calculation results. It is clear from fig. 4 (b) that the two groups of models 'dna' and 'option 2' as well as 'option 4' and 'option 5' are in good agreement with each other whether the elastic scattering or vibrational excitation and attachment are considered. It is verified that the basic cross section

models used by the two groups of models respectively are consistent. In addition, the operation time of 'option 2' and 'option 5' are less than 'dna' and 'option 5' respectively. In the case of considering elastic scattering, frequency mean lineal energy of 'option 2' and 'option 4' are lower than 'option 6', because there is not loss energy during the elastic scattering of 'option 2' and 'option 4', while the elastic scattering process is accompanied by a very small kinetic energy loss (the average deposited energy is 0.0013 eV) in 'option 6'. The mean values of 'option 2' and 'option 4' are also different because of their different elastic scattering cross section models: partial wave (PW) [36] calculations for 'option 2', and screened Rutherford (SR) formula [25] for 'option 4'. When elastic scattering is not considered, except for the small radius of the site (1 nm), the frequency mean lineal energy of 'option 6' is significantly lower than those without removing the elastic scattering process. The effect of vibrational excitation and attachment process on the frequency mean lineal energy of 'option 2' are evident when the radius is small. The cross sections of the two models are derived from the ice and water vapor data respectively [27]. When each model does not consider elastic scattering, vibrational excitation and attachment, the value of 'option 2' and 'option 4' agrees at a radius of 1 nm and 150 nm, but not much at a radius of 5 nm and 15 nm, mainly due to the difference in the relative contributions of the ionization and excitation.

Fig. 5 is the same as fig. 4 for dose mean lineal energy. It can be seen from fig. 5 that except for 'option 6', the dose mean lineal energy in some cases of other models are very close, and the results of literature [30] indicate that the dose mean lineal energy of 'option 6' has barely changed regardless of whether or not the small energy losses of elastic scattering. As the radius of the scoring sphere increases, there is a good agreement among the dose mean lineal energy of all physical processes, which is consistent with the frequency mean lineal energy. Adding the energy corresponding to several overlapping transfer points in the track, that is, considering them as one energy deposition point to be sampled, it is found that the mean lineal energy change is almost negligible.

Cut-off energy

Production cut has little influence on the mean lineal energy and interaction process of each Geant4-DNA physics constructor, while the results in the literature [30] indicate that for the microscopic volume, the production cut has a significant impact on models of the condensed-history codes (such as 'Livermore', 'Penelope'). Fig. 6 shows the effect of the tracking cut on the dose mean lineal energy. As the tracking cut increases, the mean lineal energy increases. When the set value of the tracking cut is less than the default threshold of the model, the mean lineal energy is the same as when the set value is the default threshold. It has less effect on the dose mean lineal energy when tracking cut set less than 100 eV. The mean of 'option 2' and 'option 4' is affected by the threshold to the same degree, while the mean of 'option 6' is least affected by the threshold. The trend of frequency mean lineal energy is roughly the same as dose mean lineal energy.

Fig. 7 shows number and energy percentage of excitation and ionization for monoenergetic electrons in liquid water for different tracking cuts. Tracking cut has little effect on the ionization and excitation percentage of each physical model, but it has a great influence on the energy ratio, especially for the excitation. In addition, when the set cut-off energy of track is larger than the default threshold, the influence of the energy proportion of ionization process on each physical model is consistent. Ionizing events and their energy deposition has been briefly discussed by McMahon et al. [41], and they found that the number of ionizing events determined the energy deposition enhancement in the nanoparticle, independent of any other factors.

CONCLUSION

Five different alternative physical constructors ('dna', 'option 2', 'option 4', 'option 5' and 'option 6') of Geant4-DNA toolkit were selected in this work to simulate the transport of electrons in liquid water using Geant4 run file. The number of interactions and energy of deposition of different physical constructors were analyzed for incident monoenergetic electrons with energies varying from 0.1 to 200 keV using MATLAB. Mean lineal energy were calculated in different physical constructors considering different interaction processes.

'Dna' and 'option 2' have almost identical simulation results, the same happens with 'option 4' and 'option 5', but the speed of 'option 2' and 'option 5' are faster than 'dna' and 'option 4' respectively. For the physical process, only 'dna' and 'option 2' have vibrational excitation and attachment. The effect of these two processes on frequency mean lineal energy is greater when the radius of the site is smaller, and they have no impact on dose mean lineal energy. 'Option 6' considers the very small energy loss in the elastic scattering process, making its mean lineal energy different from other physical constructors. The difference between the line energy of 'option 4' and 'option 2' is small. In addition, the production cut does not affect the lineal energy calculated by the Geant4-DNA toolkit, which would be influenced by tracking cut.

In general, 'option 2' has a wide energy range and considers more interaction processes, on account of the vibrational excitation and attachment are necessary for the simulation of electron transport down to thermalization and subsequent water radiolysis [5]. 'Option 4' was developed to correct known deficiencies of option2 (e.g. violation of sum-rules) and improved predictions on W-values (etc.) caused by the underestimation of excitations by option2, so option4 is a more accurate set of models [37]. What's more, 'option 7' is the combination of 'option 2' (>10 keV) and 'option 4' (<10 keV) [19].

The simulation of monoenergetic electrons in liquid water based on Geant4-DNA package in this work provides a powerful reference for users to select suitable models to simulate micro-scale particle transport. The monoenergetic electron data can be combined with other kinds of particles to further study the energy spectrum distribution of the complex field and provide strong support for predicting the biological effects of various types of radiation fields.

CONFLICT OF INTEREST

The authors declare that there are no conflicts of interest.

REFERENCES

1. Liamsuwan T, Emfietzoglou D, Uehara S, et al. Microdosimetry of low-energy electrons. *INT J RADIAT BIOL* 2012; 88(12): 899–907.

2. Rosenzweig W, Rossi HH. Determination of the quality of the absorbed dose delivered by monoenergetic neutrons. *RADIAT RES* 1959; 10(5): 532–44.
3. Pimblott SM, Laverne JA. Production of low-energy electrons by ionizing radiation. *Radiation Physics & Chemistry* 2007; 76(8): 1244–7.
4. Nikjoo H, Goodhead DT. Track structure analysis illustrating the prominent role of low-energy electrons in radiobiological effects of low-LET radiations. *Physics in Medicine & Biology* 1991; 36(2): 229–38.
5. Bernal MA, Bordage MC, Brown JMC, et al. Track structure modeling in liquid water: A review of the Geant4-DNA very low energy extension of the Geant4 Monte Carlo simulation toolkit. *Physica Medica* 2015; 31(8): 861–74.
6. Schulte RW, Wroe AJ, Bashkirov VA, et al. Nanodosimetry-based quality factors for radiation protection in space. *Z MED PHYS* 2008; 18(4): 286–96.
7. Nikjoo H, Uehara S, Emfietzoglou D, et al. Track-structure codes in radiation research. *RADIAT MEAS* 2006; 41(9–10): 1052–74.
8. Goodhead DT. Energy deposition stochastics and track structure: What about the target? *Radiat Prot Dosimetry* 2005; 122(1–4): 3–15.
9. Nikjoo H, Emfietzoglou D, Liamsuwan T, et al. Radiation track, DNA damage and response-a review. *REP PROG PHYS* 2016; 79(11): 116601.
10. Nikjoo H, Uehara S, Emfietzoglou D, et al. A database of frequency distributions of energy depositions in small-size targets by electrons and ions. *RADIAT PROT DOSIM* 2011; 143(2–4): 145–51.
11. Lindborg L, Nikjoo H. Microdosimetry and radiation quality determinations in radiation protection and radiation therapy. *Radiat Prot Dosimetry* 2011; 143(2–4): 402–8.
12. Moro D, Chiriotti S, Conte V, et al. Lineal energy calibration of a spherical TEPC. *RADIAT PROT DOSIM* 2015; 166(1–4): 233–7.
13. Borak TB, Doke T, Fuse T, et al. Comparisons of LET distributions for protons with energies between 50 and 200 MeV determined using a spherical tissue-equivalent proportional counter (TEPC) and a position-sensitive silicon spectrometer (RRMD-III). *RADIAT RES* 2004; 162(6): 687–92.
14. Rollet S, Colautti P, Grosswendt B, et al. Monte Carlo simulation of mini TEPC microdosimetric spectra: Influence of low energy electrons. *RADIAT MEAS* 2010; 45(10): 1330–3.
15. Arai Y, Miyoshi T, Unno Y, et al. Development of SOI pixel process technology. *Nuclear Instruments and Methods in Physics Research Section A: Accelerators, Spectrometers, Detectors and Associated Equipment* 2011; 636(1): S31–6.
16. Agostinelli S, Allison J, Amako K et al. G eant 4—a simulation toolkit. *Nuclear Instruments & Methods in Physics Research* 2003.
17. Allison J, Amako K, Apostolakis J, et al. Geant4 developments and applications. *IEEE T NUCL SCI* 2006; 53(1): 270–8.
18. Allison J, Amako K, Apostolakis J, et al. Recent developments in G eant 4. *Nuclear Instruments & Methods in Physics Research* 2016; 835(11): 186–225.
19. Incerti S, Kyriakou I, Bernal MA, et al. Geant4-DNA example applications for track structure simulations in liquid water: A report from the Geant4-DNA project. *MED PHYS* 2018; 45(8): e722–39.
20. Lindborg L, Hultqvist M, Carlsson T, et al. Lineal energy and radiation quality in radiation therapy: Model calculations and comparison with experiment. Physics in medicine & *Biology* 2013; 58(10): 3089–105.
21. Villagrasa C, Francis Z, Incerti S. Physical models implemented in the GEANT4-DNA extension of the GEANT-4 toolkit for calculating initial radiation damage at the molecular level. *RADIAT PROT DOSIM* 2011; 143(2–4): 214–8.
22. Incerti S, Ivanchenko AM, Mantero A, et al. Comparison of GEANT4 very low energy cross section models with experimental data in water. *MED PHYS* 2010; 37(9): 4692–708.
23. Lillh K JE, J-E G, Lindborg L, et al. Nanodosimetry in a clinical neutron therapy beam using the variance-covariance method and Monte Carlo simulations. *Physics in Medicine & Biology* 2007; 52(16): 4953–66.
24. Nikjoo H, Uehara S. Comparison of various Monte Carlo track structure codes for energetic electrons in gaseous and liquid water. *Basic Life Sciences* 1994;63:167.
25. Uehara S, Nikjoo H, Goodhead DT. Cross-sections for water vapour for the Monte Carlo electron track structure code from 10 eV to the MeV region. *Physics in Medicine & Biology* 1993; 38(12): 1841.
26. Francis Z, Incerti S, Ivanchenko V, et al. Monte Carlo simulation of energy-deposit clustering for ions of the same LET in liquid water. *Physics in Medicine & Biology* 2012; 57(1): 209–24.
27. Francis Z, Incerti S, Capra R, et al. Molecular scale track structure simulations in liquid water using the Geant4-DNA Monte-Carlo processes. *Applied Radiation & Isotopes Including Data Instrumentation & Methods for Use in Agriculture Industry & Medicine* 2011; 69(1): 220–6.
28. Emfietzoglou D, Papamichael G, Nikjoo H. Monte Carlo electron track structure calculations in liquid water using a new model dielectric response function. *RADIAT RES* 2017; 188(3).
29. Kyriakou I, Šefl M, Nourry V, et al. The impact of new Geant4-DNA cross section models on electron track structure simulations in liquid water. *J APPL PHYS* 2016; 119(19): 194902.
30. Kyriakou I, Emfietzoglou D, Ivanchenko V, et al. Microdosimetry of electrons in liquid water using the low-energy models of Geant4. *J APPL PHYS* 2017; 122(2): 24303.
31. Kyriakou I, Ivanchenko V, Sakata D et al. Influence of track structure and condensed history physics models of Geant4 to nanoscale electron transport in liquid water. *Physica Medica* 2019;58:149–54.
32. Lazarakis P, Incerti S, Ivanchenko V, et al. Investigation of track structure and condensed history physics models for applications in radiation dosimetry on a micro and nano scale in Geant4. *Biomedical Physics & Engineering Express* 2018; 4(2): 24001.
33. Bordage MC, Bordes J, Edel S, et al. Implementation of new physics models for low energy electrons in liquid water in Geant4-DNA. *Physica Medica* 2016; 32(12): 1833–40.

34. Kim YK, Rudd ME. Binary-encounter-dipole model for electron-impact ionization. *PHYS REV A* 1994; 50(5): 3954.
35. Basaglia T, Han MC, Hoff G, et al. Experimental quantification of Geant4 PhysicsList recommendations: Methods and results. *Journal of Physics: Conference Series* 2015; 664(7): 72037.
36. Champion C, Incerti S, Aouchiche H, et al. A free-parameter theoretical model for describing the electron elastic scattering in water in the Geant4 toolkit. *RADIAT PHYS CHEM* 2009; 78(9): 745–50.
37. Kyriakou I, Incerti S, Francis Z. Technical note: Improvements in geant4 energy-loss model and the effect on low-energy electron transport in liquid water. *MED PHYS* 2015; 42(7): 3870–6.
38. Emfietzoglou D. Inelastic cross-sections for electron transport in liquid water: A comparison of dielectric models. *Radiation Physics & Chemistry* 2003; 66(6): 373–85.
39. Emfietzoglou D, Nikjoo H. The effect of model approximations on single-collision distributions of low-energy electrons in liquid water. *RADIAT RES* 2005; 163(1): 98–111.
40. Kellerer AM, Chmelevsky D. Concepts of microdosimetry. III. Mean values of the microdosimetric distributions. *Radiat Environ Biophys* 1975; 12(4): 321–35.
41. Mcmahon SJ, Hyland WB, Muir MF, et al. Biological consequences of nanoscale energy deposition near irradiated heavy atom nanoparticles. *Sci Rep* 2011; 1(6): 18.